

414. A numerical study of the existence and stability of some chaotic attractors by path integration

A. Naess^{1,a}, E. Mo^{2,b}

¹ Centre for Ships and Ocean Structures & Department of Mathematical Sciences
Norwegian University of Science and Technology, Trondheim, Norway

² Sonowand, Trondheim, Norway

e-mail: ^aarvidn@math.ntnu.no, ^beirik.mo@sonowand.no

(Received: 19 September; accepted: 02 December)

Abstract. The response of a harmonically excited Duffing oscillator with chaotic response is studied by replacing the excitation by harmonic excitation plus added noise, a harmonic motion with phase perturbations, and a narrow-band filtered noise. The mean frequency and excitation energy for all the models are the same, assuming that these are basic parameters for the response of the oscillator. The resulting probability densities in the state space show that the chaotic attractor is very stable for the different kinds of perturbations. Also, a new conditional path integration method is described, which is shown to be robust and accurate while the CPU time is kept at a minimum.

Keywords: chaotic attractor, additive noise, random phase modulation, path integration, probability density function.

Introduction

A few papers have been published the last years with studies of nonlinear or chaotic systems under the influence of noise - or other kinds of perturbations, and a variety of phenomena has been discovered. There are however many ways noise can be introduced, and very little has been done to look at differences between the response under various noise models.

The aim of this paper is to show some of the possibilities of using path integration for systems where the noise is filtered, increasing the dimensionality of the problem to four, when a state-space variable is an angle. Although the systems considered have some very basic properties in common, the notion of convergence and how the attractor finally appears are very different for the different cases. This paper also extends previous work [1,2] where a single-degree of freedom ODE with chaotic response is studied by the addition of noise using path integration.

The Duffing oscillator has been studied extensively for many years because of its interesting dynamics combined with its simplicity, and it is still recognized that the Duffing class of oscillators plays a central role among harmonically excited systems that exhibit chaotic behaviour [3]. Parameter ranges for different structure levels has been mapped quite detailed, e.g. in [4], and the Duffing model is also used to model more complicated structures of coupled nonlinear oscillators [5]. As the deterministic single-degree-of-freedom oscillator is more understood, the interest is turned to stochastic models and higher-dimensional problems.

Path integration (PI) is one tool for analyzing systems of SDEs. A Duffing oscillator with additive noise was studied using PI in [6]. Their method is very different from the

method developed by Naess and described i.e. in [7], and with different limitations. The first is based on an idea described in [8], where moment equations are solved using the Gaussian closure technique to estimate the transition probability density (TPD) using fairly long time steps. The TPD multiplied with the PDF of the previous time step is then integrated using a Gauss-Legendre interpolation scheme, though with only two sub-intervals in each grid point. The longer time steps and direct evaluation of the PDF in the pre-defined grid points is computer efficient, at least for two-dimensional problems. The idea of Naess is, as will be discussed below, to take shorter time steps, and use a time discretization scheme where the noise has a known distribution and only appear in one variable of the discretized system of one-dimensional SDEs. This requires an efficient and accurate interpolation method over the density integrated over, but is more robust to non-Gaussian long-term TPDs which occur in strongly nonlinear systems. One important remark to the method presented in this paper, is that it is a very direct implementation. Some methods have been proposed for solving or studying nonlinear SDEs subjected to narrow-band random excitation involves the quasi-static method [9], stochastic averaging [10], equivalent linearization [11,12] and digital simulations [13], just to mention a few. These requires more involved analytical computations or adjustments before one can start simulations of the systems.

System description

A nonlinear single-degree-of-freedom (SDOF) system subject to periodic excitation is the basis for this analysis. This system is a Duffing oscillator where the response process $X(t)$ satisfies the following equation

$$\ddot{X}_t + \frac{1}{25}\dot{X}_t - \frac{1}{5}X_t + \frac{8}{15}X_t^3 = F(t), \quad (1)$$

where $F(t)$ is the stochastic excitation, with some specific properties. The motivation for this study is the corresponding deterministic ODE with $Y(t) = (2/5)\cos(\Omega t)$, which has been studied extensively in [14] for various frequencies Ω .

This system is separated into displacement X and velocity V as

$$\dot{X}_t = V_t \quad (2)$$

$$\dot{V}_t = -\frac{1}{25}V_t + \frac{1}{5}X_t - \frac{8}{15}X_t^3 + F(t). \quad (3)$$

The four kinds of excitation studied here, denoted A through D are

$$F_A(t) = \frac{2}{5}\cos(\Omega t) + \gamma_A N_t, \quad (4)$$

$$F_B(t) = \frac{2}{5}\cos(\Omega t + \Phi_t), \dot{\Phi}_t = -k_B \Phi_t + \gamma_B N_t, \quad (5)$$

$$F_C(t) = \frac{2}{5}\cos(\Theta_t), \dot{\Theta}_t = \Omega + \gamma_C N_t, \quad (6)$$

$$F_D(t) = Z_t \ddot{Z}_t + k_D \Omega \dot{Z}_t + \Omega^2 Z_t = \gamma_D N_t. \quad (7)$$

Here, N_t is the standard zero-mean white noise process or Gaussian white noise, also described as the formal derivative of a standard one-dimensional Brownian motion. This process has uncorrelated increments $E[N_t N_{t+\tau}] = \delta(\tau)$, where $\delta(\cdot)$ is a Dirac measure at zero.

As in equation 2, the filter in case D will be split into two first-order SDEs by introducing the filter velocity $W = \dot{Z}$.

From here on, Y will be the vector of state space variables, which for the four cases read

$$Y_A = [X, V]^T \in R^2 \quad (8)$$

$$Y_B = [X, V, \Phi]^T \in R^3 \quad (9)$$

$$Y_C = [X, V, \Theta]^T \in R^2 \times S \quad (10)$$

$$Y_D = [X, V, Z, W]^T \in R^4 \quad (11)$$

Here S denotes the circle; the real line modulo 2π .

The differences between the two three-dimensional systems B and C require a comment. Both are models where there is a perturbation in the frequency of the forcing, while preserving the mean angular velocity around Ω . In case B, the system is almost locked to a fixed phase at every time t , perturbed by Φ . Although Φ is strictly an angle, the noise variance is set small enough that the perturbation is much less than 2π . By this, it is reasonable to model this variable and the Brownian motion as a one-dimensional process on the real line. This also ensures that the forcing cannot stay a full period behind or ahead of the

pre-set phase. In a realization of the system, any random delay compared to that phase at a specific time would make the damping effect try to "speed up" the angle, and the more the angle is ahead of the phase due to the random fluctuations, the larger the probability is for dominating lower frequencies. In case C, the filter does not inherit this kind of memory. The angle can be seen as a standard zero-mean Brownian motion on a circle superimposed on a fixed rotation, or a Brownian motion on the circle with a mean angular velocity, or say drift, Ω . As the variance of the Brownian motion on the real line is increasing with time, the distribution on the circle converges towards a uniform distribution, which means that the phase for system C after a long time is impossible to predict with any accuracy, in contrast to system B. However, the value of Θ is the current phase value.

The spectrum of F_C in Equation 6 is, according to [15],

$$S(\omega) = \frac{1}{2} \frac{(2/5)^2 \gamma_D^2 (\Omega^2 + \omega^2 + \gamma_D^4 / 4)}{(\Omega^2 - \omega^2 + \gamma_D^4 / 4)^2 + \omega^2 \gamma_D^4}. \quad (12)$$

This also shows the fairly obvious result that $\gamma_D \rightarrow 0$ gives harmonic excitation.

The fourth filter, D, is an oscillator that also gives a mean frequency Ω . As in case C, the phase will be distributed over the joint PDF, but can be retained from the values of the two last state variables. Here, the amplitude will also be heavily affected by the noise. The output of a linear filter with Gaussian noise is Gaussian, so the forcing spectrum is clearly different from the sinusoidal in the three first cases.

It is known that the purely deterministic system with harmonic forcing, $\gamma_A = 0$ in Equation (4), gives rise to a chaotic attractor. With all the noise models, it is expected that the response should be similar to this attractor, more so for noise with low intensity. As the noise makes a probability density, i.e. a surface, some of the fine structure of the chaotic attractor must disappear, like a "stochastic blanket" is thrown over the attractor.

To be a relevant comparison, approximately the same amplitude should be delivered from the stochastic forcing models. This is clearly a question of definition, e.g. would the addition of zero-mean noise in case A give an addition in energy and mean amplitude, but a time average around the peaks would give the correct amplitude. For cases B and C, the amplitude is fixed, but the frequency variation would give a slight increase in energy to the system. In the last case D, a choice has to be made, as the force is just quasi-harmonic without a maximum amplitude. Here, the variance was chosen as the reference. The variance in Z of the system D is from equation (7) $\gamma_D^2 / (2\Omega^3 k_D)$. The variance of the deterministic forcing $(2/5)\cos(\Omega t)$ is $2/25$. If these two are set equal to each other, a given damping k_D implies a noise level $\gamma_D^2 = 4\Omega^3 k_D / 25$. This is equivalent to scaling the forcing in equation (2). As the damping and noise intensity goes to zero, the response Z becomes more and more harmonic, as shown in Figure 1.

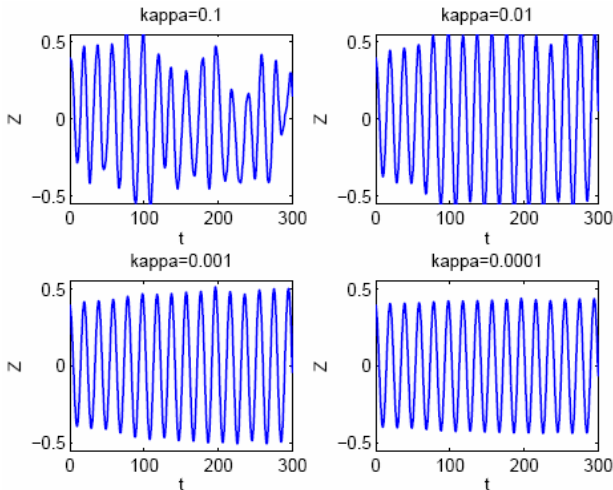


Fig. 1. Four realizations of the two-dimensional filter with damping k_D varying from 0.1 down to 0.0001, and noise level chosen correspondingly

The concept of convergence for SDEs driven by harmonic excitation has been discussed in [2]. For the two first excitation models *A* and *B*, the response is directly depending on the value of the time t . Since the damping is positive, it can be assumed that the density becomes periodic after transients have died out, and the period will be $2\pi/\Omega$. Existence and uniqueness of such a periodic attractor for the response PDF is difficult to prove for a nonlinear system. However, if a PDF f^\dagger at time t_0 is found to be periodic with period $2\pi n/\Omega$, then the density f^\dagger obtained at time $t_1 = t_2 + 2\pi/\Omega$ also has the same period. The average over all the obtained PDFs at $t_1, t_2, \dots, t_n, t_j = t_1 + 2\pi j/\Omega$ must then have period $2\pi/\Omega$.

For the third and fourth cases, there is no explicit time dependence; the system is autonomous, and a stationary distribution could exist.

The Path Integration Method

The vector SDE for the n -dimensional state space vector is

$$\dot{Y}(t) = m[Y(t)] + b\xi(t) \tag{13}$$

Let $p_Y(y, t)$ denote the PDF of Y at time t . To solve the SDE (13), the PI technique is used. It is based on the total probability law, which reads

$$p_Y(y, t) = \int_{-\infty}^{\infty} \dots \int_{-\infty}^{\infty} p(y, t | y', t') p_Y(y', t') dy'_1 \dots dy'_n, \tag{14}$$

This means that for each point y , the value of the PDF at time t can be calculated as an integral based on the previous PDF at time $t' = t - \Delta t$, if the path between the points y and y' in the state space can be calculated. Time can therefore be discretized with constant time steps Δt using the fourth order Runge-Kutta scheme (RK4).

The integral in Equation (14) requires the (incremental)

transition probability density (TPD). For a sufficiently small Δt , this is a degenerate Gaussian distribution

$$p(y, t | y', t') = \prod_{i=1}^{n-1} \delta(y_i - y'_i - r_i(y')\Delta t) \tag{15}$$

$$\cdot \frac{1}{\sqrt{2\pi\sigma^2\Delta t}} \exp\left(-\frac{(y_n - y'_n - r_n(y')\Delta t)^2}{2\sigma^2\Delta t}\right),$$

where $r_j(y')\Delta t, j = 1, 2, \dots, n$ are the RK4 increments for y_1, y_2 to y_n , respectively. That is, m_j has been replaced by r_j in the discretized version of the SDE (13). Note that due to the occurrence of the delta functions in the expression for the TPD $p(y, t | y', t')$ in equation (15), the integrals in equation (14) will be reduced to a single integral, cf. [7]. This is a significant remark, especially for the four-dimensional problem. An integral over all the state space variables, which would appear with a higher order time-discretization of the SDE or the use of moment equations, would be very time consuming.

To evaluate the PDF at time t' , a cubic B-spline interpolation [16] is used, made especially as a tensor product over the state space. This is an efficient choice, as the spline coefficients of a surface is represented by the spline coefficients in one direction of the spline coefficients in the second direction, and the value of a two-dimensional B-spline basis function is the product of the corresponding basis functions in the two directions. This argument could similarly be extended to higher dimensions. As will be discussed below, interpolating on a conditional density makes linear interpolation acceptable for some systems.

For the results obtained in this paper, a uniform grid has been used, which leads to splines with periodic blending functions. For all the systems, the PDF fall off to zero when one of the state space variables gets sufficiently far from the origin. The simplest endpoint condition numerically is to set the coefficient to zero for all basis functions with the peak outside the computation domain. This also leads to an interpolant that smoothly goes to zero at the boundary of the domain, which seems reasonable for the systems studied here. The system to be solved in each state space variable is then

$$\frac{1}{6} \begin{bmatrix} 4 & 1 & 0 & \dots & 0 & 0 \\ 1 & 4 & 1 & \ddots & 0 & 0 \\ 0 & 1 & 4 & \ddots & 0 & 0 \\ \vdots & \ddots & \ddots & \ddots & \vdots & \vdots \\ 0 & 0 & 0 & \ddots & 4 & 1 \\ 0 & 0 & 0 & \dots & 1 & 4 \end{bmatrix} \begin{bmatrix} c_1 \\ c_2 \\ c_3 \\ \vdots \\ c_{N-1} \\ c_N \end{bmatrix} = \begin{bmatrix} v_1 \\ v_2 \\ v_3 \\ \vdots \\ v_{N-1} \\ v_N \end{bmatrix}, \tag{16}$$

where the vector $[c_1, \dots, c_N]^T$ is the spline coefficients and $[v_1, \dots, v_N]^T$ contains the PDF values.

The splines in case C have a bit different properties, as the state space includes S . In the discretized space the Θ

variable has the same number of basis splines and knots as there are values to interpolate, as the spline coefficients are fully determined under the periodic endpoint conditions of the space. The spline matrix system to be inverted is

$$\frac{1}{6} \begin{bmatrix} 4 & 1 & 0 & \cdots & 0 & 1 \\ 1 & 4 & 1 & \ddots & 0 & 0 \\ 0 & 1 & 4 & \ddots & 0 & 0 \\ \vdots & \ddots & \ddots & \ddots & \vdots & \vdots \\ 0 & 0 & 0 & \ddots & 4 & 1 \\ 1 & 0 & 0 & \cdots & 1 & 4 \end{bmatrix} \begin{bmatrix} c_1 \\ c_2 \\ c_3 \\ \vdots \\ c_{N-1} \\ c_N \end{bmatrix} = \begin{bmatrix} v_1 \\ v_2 \\ v_3 \\ \vdots \\ v_{N-1} \\ v_N \end{bmatrix}, \quad (17)$$

So the only change is in the upper right and lower left corner of the matrix. In any case, the spline coefficient vector is found by one initial LU-decomposition of the matrices above, and back substitution at every time step.

The chaotic attractor of the deterministic system described above is a complicated structure in three dimensions, x , \dot{x} or v , and time or phase angle. For the two non-autonomous systems A and B, the latter variable is represented by the time steps, and hence the accuracy depends on the size of the time step and the time stepping method. For the two cases C and D, however, the grid needs to be sufficiently dense in all dimensions to see the fine structure of the system. That is, in case C where Θ , the phase angle, is a state space variable, it cannot be regarded as less important than the two first, even if it will not be shown in the main results. This is basically irrespective of the order of the interpolation scheme, as both a linear and a cubic B-spline interpolant will smear out the attractor's fine structure.

Conditional Path Integration

With the increase of computer power, also systems of higher dimensions can be studied. However, most work on path integration deals with one- or two-dimensional systems. The main obstacle and challenge with the PI method is the interpolation in many dimensions, because it requires a lot of programming, and it is the bottleneck for the CPU-time. An additional pitfall is that in higher dimensions the accuracy of the interpolation is lower than in one-dimensional systems.

For case B, the stationary density of the Φ_t process is Gaussian with density $f(\phi) = C \exp(-k_B x^2 / \gamma_B^2)$, i.e. zero mean and variance $\gamma_B^2 / 2k_B$. (C is just the constant scaling). The marginal PDF of Φ from X, V, Φ must also be the same Gaussian distribution, as the three-dimensional system only has introduced "auxiliary" variables X and V and then they are integrated out for the marginal. In case D, the joint stationary - and marginal - PDF of Z, W is bivariate Gaussian with density $f(z, \omega) = C \exp(-k_D \Omega / \gamma_D^2 [\Omega^2 z^2 + \omega^2])$. That is, zero-mean, zero covariance, and variances $\gamma_D^2 / (2\Omega^3 k_D)$ and $\gamma_D^2 / (2\Omega k_D)$ for the

response of Z and W respectively.

The question is whether this knowledge could be utilized to reduce both the grid resolution and the interpolation cost. A proposed solution is to consider the conditional densities $f(x, v / \phi)$ and $f(x, v / z, \omega)$ for these two cases respectively, and just interpolate linearly in the conditional variables. This will work well if the conditional density $f(\phi / x, v)$ for fixed x, v has a sufficiently similar shape to $f(\phi)$ in case B, and similarly for case D.

Let us go through the procedure for case B in detail. Assume that the PDF $f_{i\Delta}(y)$ is already calculated in every grid point $y_{k,l,m}$ and denote this for short by $f_i(y)$. Write $f_i(x_k, v_l / \phi_m) = f_i(y_{k,l,m}) / f(\phi_m)$ for every grid point. For each fixed m , represent f_i by the cubic spline interpolant $g_m(x, v) = (I_{4,x,v} f_i)(x, v / \phi_m)$. For each point in the integration domain the density is evaluated as

$$f_i(x, v, \phi) = [(1 - \lambda_m)g_m(x, v) + \lambda_m g_{m+1}(x, v)] f(\phi), \text{ where } \lambda_m = \lambda_m(\phi) = (\phi - \phi_m) / (\phi_{m+1} - \phi_m), \text{ and } m \text{ is chosen such that } \phi_m < \phi < \phi_{m+1}.$$

In case D, the method is the same, except more in

$$f_i(x, v, z, \omega) = [(1 - \lambda_m)(1 - \lambda_n)g_{m,n}(x, v) + \lambda_m(1 - \lambda_n)g_{m+1,n}(x, v) + (1 - \lambda_m)\lambda_n g_{m,n+1}(x, v) + \lambda_m \lambda_n g_{m+1,n+1}(x, v)] f(z, \omega). \quad (18)$$

A challenge with this fourth four-dimensional system, is that the filter has a transient time, which is very long for low noise levels. The main attempt to reduce this is by starting with the correct marginal density in Z and \dot{Z} .

A final remark on conditional PI is that the procedure could also work for systems where the marginal density of the filter variables is unknown or not stationary, as this PDF can also be found for each time step with fair accuracy using the PI method.

Numerical solution for response PDF by the PI method

A Poincare section of the chaotic attractor obtained for the deterministic system, case A with $\gamma_A = 0$ in Equation (4) is shown in Figure 2. This is a well studied example, using $\Omega = 0.32$, and this choice has been made for all the simulations with results shown in this paper. The sampling time is $2\pi k / \Omega$, $k = 1, 2, \dots$, i.e. after every full period of the harmonic forcing.

Snapshots of the PDF of the additive noise model A, Equation (4), after 30 periods are shown in Figures 3 to 8, for experiments with varying amount of noise. As expected, the higher noise levels give less fine structure and more spreading of the PDF. There is hardly any difference between the estimated response for the two lowest noise levels. This could indicate that for these results, at least for the lowest noise level, the interpolation is the main source of smearing out the attractor, and the

limit of structure detail obtainable has been reached. It is also interesting to see that the strongest peak at the upper left tip of the structure gradually becomes lower with increasing noise, while the vertical structure around $x = 1.5$ remains strong. Similarly, one of two peaks near the center of the figures gradually disappear with increasing noise, while the other remains a maxima.

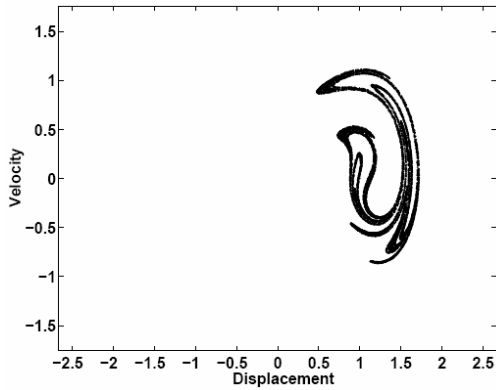


Fig. 2. Poincaré section of the chaotic attractor

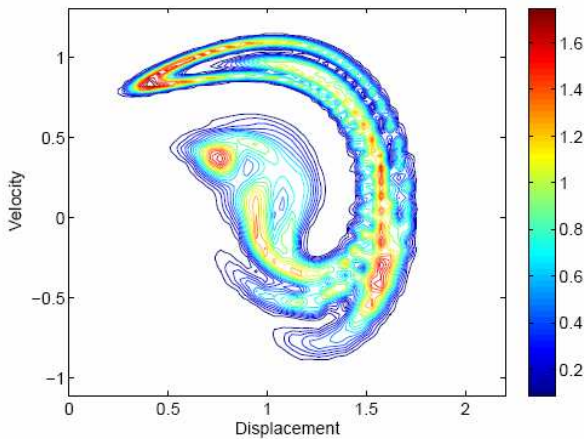


Fig. 3. PDF of the response of the 2D system, additive noise, with $\gamma_A = 0.005$ at time $60\pi/\Omega$, i.e. 30 full periods from the initial distribution

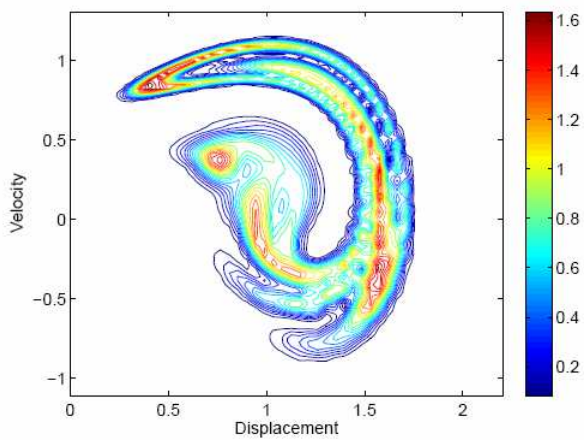


Fig. 4. PDF of the response of the 2D system, additive noise, with $\gamma_A = 0.010$ at time $60\pi/\Omega$, i.e. 30 full periods from the initial distribution

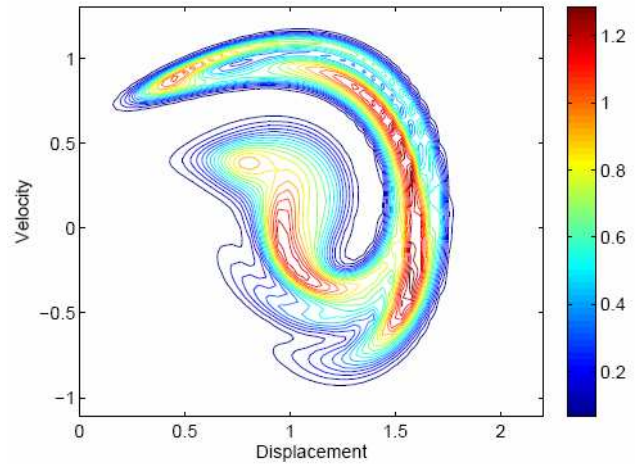


Fig. 5. PDF of the response of the 2D system, additive noise, with $\gamma_A = 0.025$ at time $60\pi/\Omega$, i.e. 30 full periods from the initial distribution

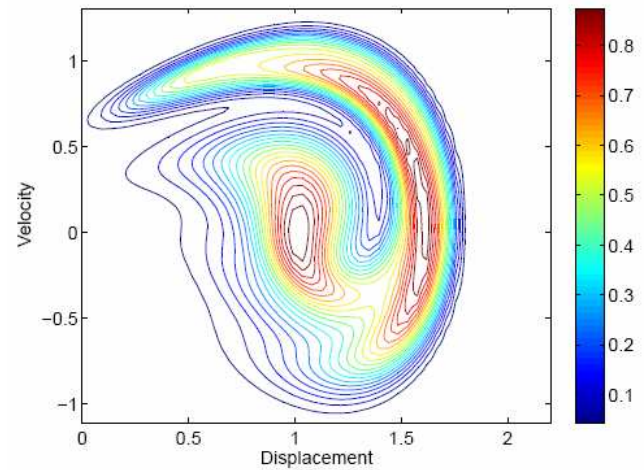


Fig. 6. PDF of the response of the 2D system, additive noise, with $\gamma_A = 0.050$ at time $60\pi/\Omega$, i.e. 30 full periods from the initial distribution

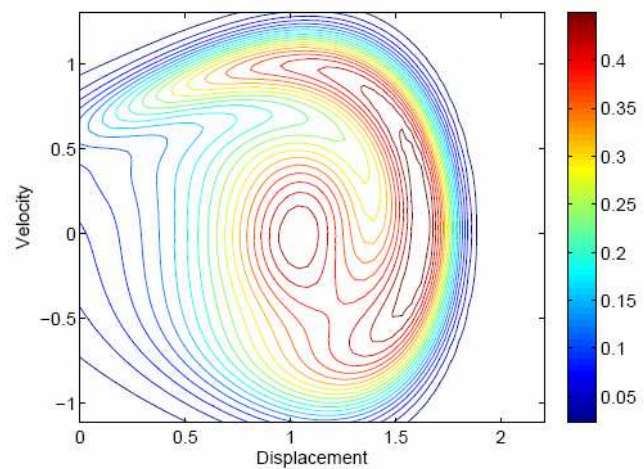


Fig. 7. PDF of the response of the 2D system, additive noise, with $\gamma_A = 0.100$ at time $60\pi/\Omega$, i.e. 30 full periods from the initial distribution

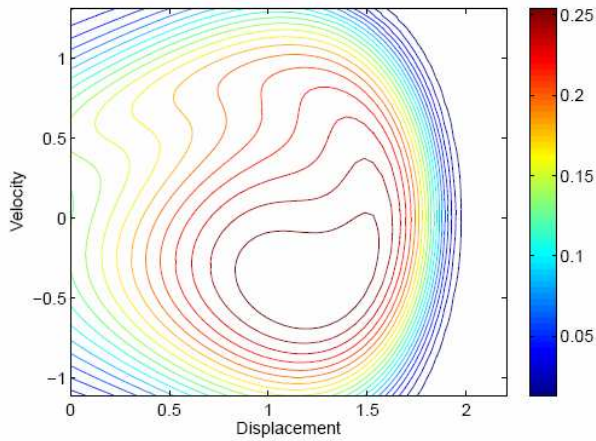


Fig. 8. PDF of the response of the 2D system, additive noise, with $\gamma_A = 0.250$ at time $60\pi/\Omega$, i.e. 30 full periods from the initial distribution

Similar snapshots are shown for system B in Figures 9 through 13. In spite of the fact that the phase is varying and the amplitude is constant, while case A is opposite, the increasing noise seem to have the same effect on the system.

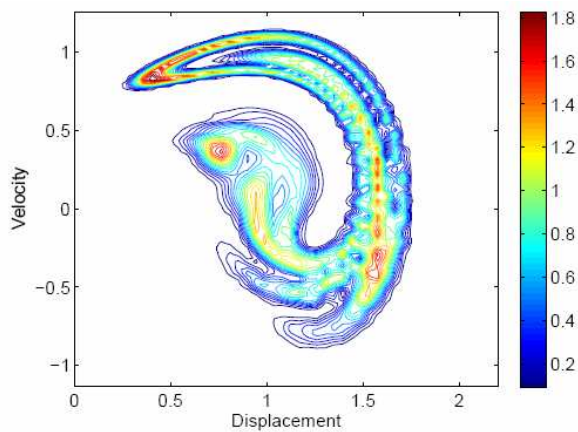


Fig. 9. PDF of the response of the 3D system, damped noise in the phase, with $\gamma_B = 0.005$ at time $60\pi/\Omega$, i.e. 30 full periods from the initial distribution

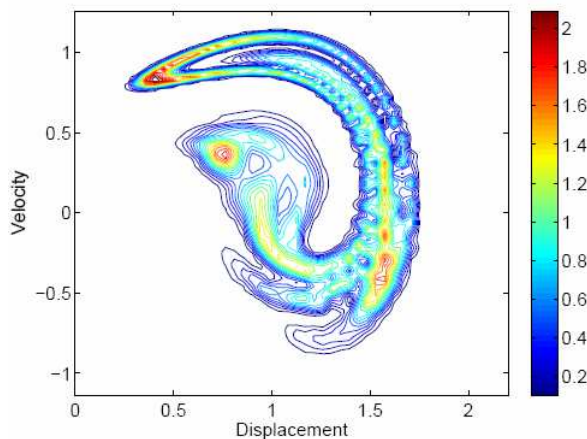


Fig. 10. PDF of the response of the 3D system, damped noise in the phase, with $\gamma_B = 0.010$ at time $60\pi/\Omega$, i.e. 30 full periods from the initial distribution

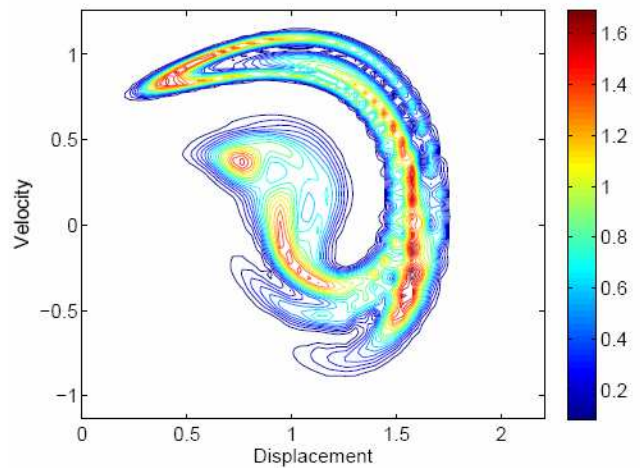


Fig. 11. PDF of the response of the 3D system, damped noise in the phase, with $\gamma_B = 0.050$ at time $60\pi/\Omega$, i.e. 30 full periods from the initial distribution

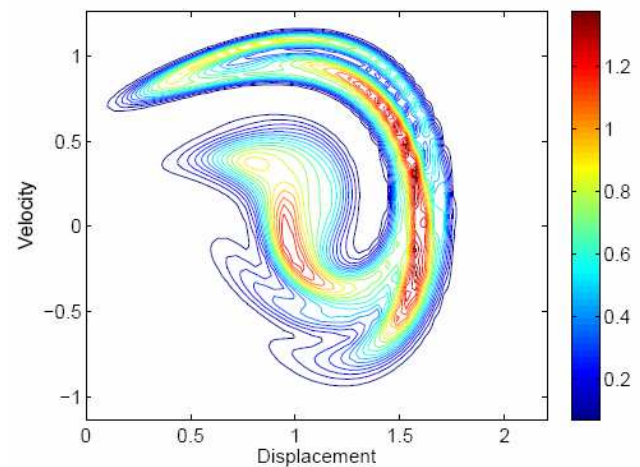


Fig. 12. PDF of the response of the 3D system, damped noise in the phase, with $\gamma_B = 0.100$ at time $60\pi/\Omega$, i.e. 30 full periods from the initial distribution

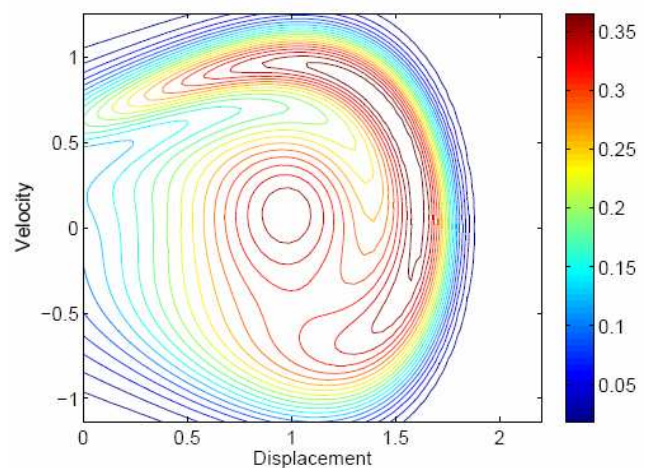


Fig. 13. PDF of the response of the 3D system, damped noise in the phase, with $\gamma_B = 0.500$ at time $60\pi/\Omega$, i.e. 30 full periods from the initial distribution

For the filtered noise version, case D, the results are shown in Figures 19 to 21. Even for the low damping, and hence low noise, one cannot see the same level of detail as in the previous results. This indicates that some averaging process is dominant for this system much more than for the previous cases. The location and size of the maxima is similar to what is seen for high noise levels in the other models. When studying the two Figures 19 and 20, it is

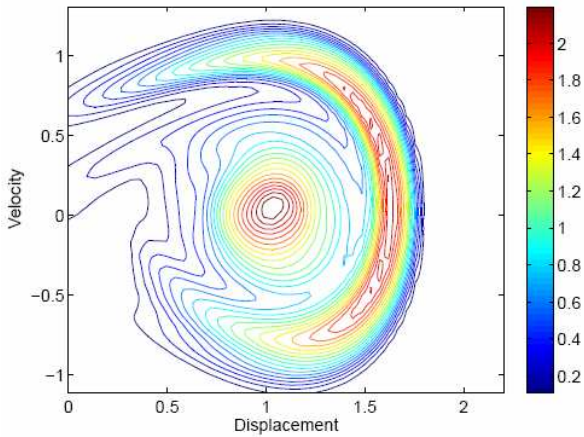


Fig. 14. PDF of the response of the second 3D system, free noise in the phase, with $\gamma_C = 0.005$. Number of grid points in Θ is 22

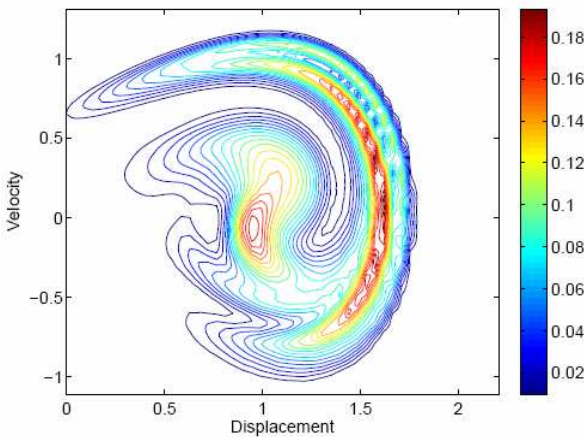


Fig. 15. PDF of the response of the second 3D system, free noise in the phase, with $\gamma_C = 0.005$. Number of grid points in Θ is 44

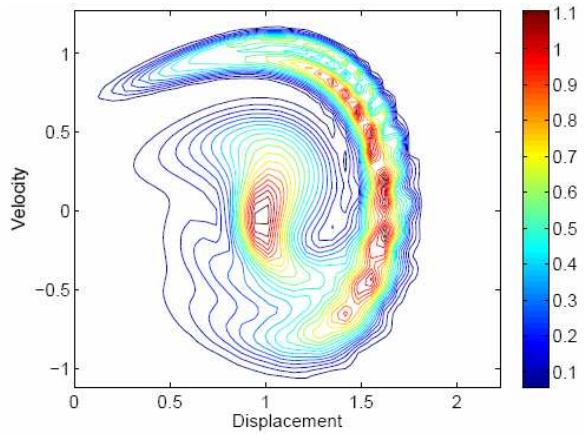


Fig. 16. PDF of the response of the second 3D system, free noise in the phase, with $\gamma_C = 0.050$. Number of grid points in Θ is 88, while the number of grid points in x and y is reduced by 2/3 to 81

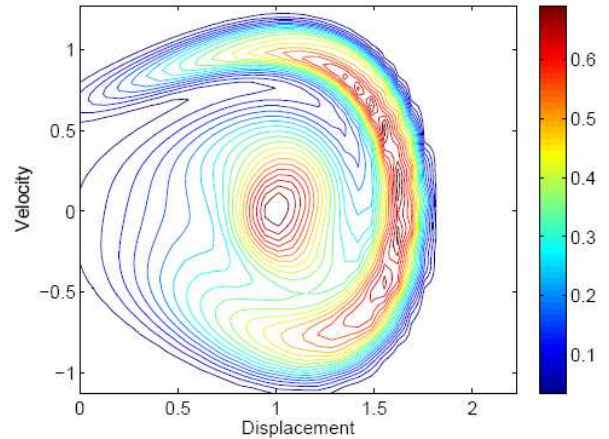


Fig. 17. PDF of the response of the second 3D system, free noise in the phase, with $\gamma_C = 0.100$. Number of grid points in Θ is 88, while the number of grid points in x and y is reduced by 2/3 to 81

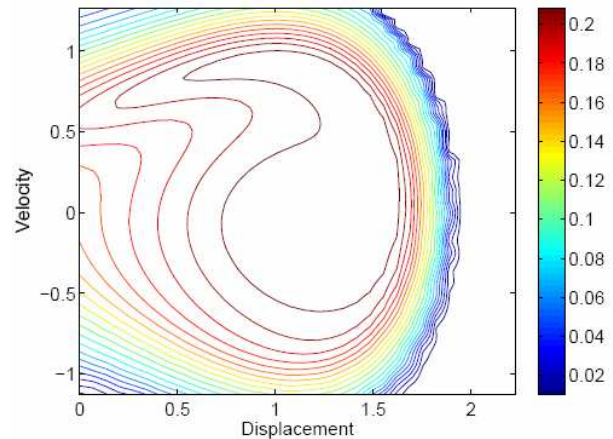


Fig. 18. PDF of the response of the second 3D system, free noise in the phase, with $\gamma_C = 0.500$. Number of grid points in Θ is 88, while the number of grid points in x and y is reduced by 2/3 to 81

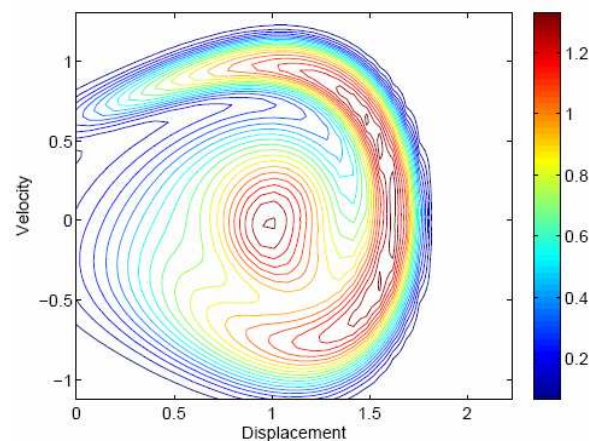


Fig. 19. PDF of the response of the 4D system, filtered noise, with $k_D = 0.0001$

quite surprising that the PDF doesn't seem to change when the damping is increased from 10^{-4} to 10^{-1} , as the realizations of the forcing shown in Figure 1 are so different. Simulations were performed with a grid of

81×81×44×45 grid points over the state space. In the z -direction, the grid was from -0.8 to 0.8, i.e. twice the value of interest, 0.4. The grid for the ω -direction was chosen correspondingly based on the maximal velocity (0.4Ω). As discussed above, the deterministic harmonic forcing corresponds to an ellipse in the z, ω -space. With the choice of computational grid, this ellipse crosses 22 grid lines in each direction - twice, so the interpolation was expected to be fairly good. It is possible that interpolation in four dimensions smears out the structure much more than in the previous cases, also since just two points on the ellipse actually intersects grid points. Also note that the separation between the two peaks is clearly decreased as the noise increases, while the main shape is preserved. For the case with highest damping and noise, Figure 21, very little shape is preserved, the maxima is almost circular, although the total variation is about the same as in Figure 18 and Figures 8, and not much larger than in 13, all of which has a clearly non-circular maximum. However, the added noise model is much more similar to the 4D case than the two 3D models. This clearly indicates that the filtered noise model and the added noise model affect the oscillator in a very different way than the phase perturbation for high noise values.

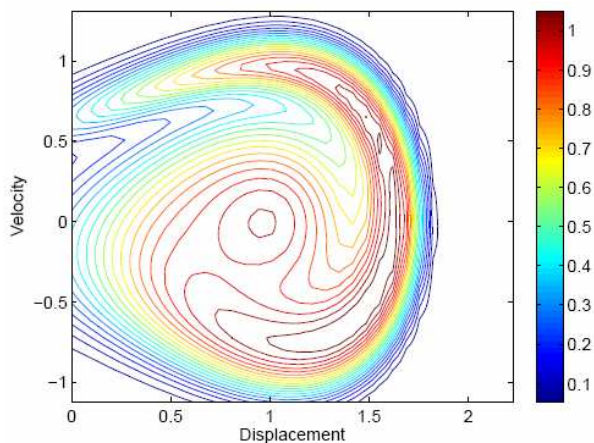


Fig. 20. PDF of the response of the 4D system, filtered noise, with $k_D = 0.10$

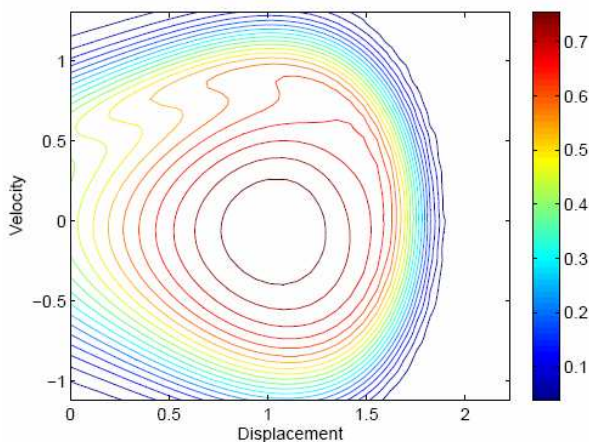


Fig. 21. PDF of the response of the 4D system, filtered noise, with $k_D = 1.0$

Conclusion

Two slightly modified versions of the path integration method is presented; a conditional routine to reduce cpu-time, and a way to treat periodic boundary conditions when the variable with noise is an angle. These methods are used to study the behaviour of a nonlinear system excited by a harmonic motion with additive noise, two different models with slowly varying phase, and a filtered noise process. The PDF for the response of the system is obtained numerically for all these excitation types, and with varying amount of noise. The pure deterministic system is known to produce a chaotic periodic attractor, and the main location of this attractor seems to be stable in the different stochastic models, although the level of detail varies.

The paper shows that low levels of noise combined with a dense grid gives a lot of detail or structure in the resulting PDFs. This structure becomes more spread out and less detailed as the noise level is increased or fewer grid points are used in the interpolation. It is shown that for the PI technique, all the variables must be represented by a sufficiently accurate discretization technique to obtain a detailed final accuracy.

The conditional path integration is a new method presented here, based on the knowledge of the stationary distribution in some of the variables. This gives faster computation time, and preserves the marginal density of the full PDF. At the same time, one to a large extent avoids the main drawback of linear interpolation in PI, namely consistent under-estimation of peaks, i.e. in areas with negative curvature, and similarly over-estimation of tails.

The Path Integration technique is able to produce full PDFs of even four-dimensional nonlinear systems, and with our interpretation, the results are reasonable.

Acknowledgements

This work has been supported by the Research Council of Norway.

REFERENCES

- [1] **A. Naess** Chaos and nonlinear stochastic dynamics. *Probabilistic Engineering Mechanics*, 15(1):37-47, 2000.
- [2] **A. Naess and C. Skaug** *The study of chaotic attractors of nonlinear systems by path integration*, chapter Namachivaya, N.S. and Lin Y.K. (eds), pages 445-454. Proceedings of the IU-TAM Symposium on Nonlinear Stochastic Dynamics, Monticello, Illinois, USA, August 2002. Kluwer Academic Publishers, Dordrecht, 2002.
- [3] **Ph. Holmes** A nonlinear oscillator with a strange attractor. *Phil. Trans. of the Royal Society, London*, A292:419-448, 1979.
- [4] **R. Gilmore and J.W.L. McCallum** Structure in the bifurcation diagram of the Duffing oscillator. *Physical Review E*, 51(2):935-956, 1995.
- [5] **D.E. Musielak, Z.E. Musielak, and J.W. Benner** Chaos and routes to chaos in coupled Duffing oscillators with multiple degrees of freedom. *Chaos, Solitons and Fractals*, 24:907-922, 2005.

- [6] **J.S. Yu and Y.K. Lin** Numerical path integration of a non-homogeneous Markov process. *Int. J. of Non-Linear Mechanics*, 39:1493-1500, 2004.
- [7] **A. Naess and V. Moe** Efficient path integration methods for nonlinear dynamic systems. *Probabilistic Engineering Mechanics*, 15(3):221-231, 2000.
- [8] **J.S. Yu, G.Q. Cai, and Y.K. Lin** A new path integration procedure based on Gauss- Legendre scheme. *Int. J. Non-Linear Mechanics*, 32(4):759-768, 1997.
- [9] **M. Grigoriu** Probabilistic analysis of response of Duffing oscillator to narrow band stationary Gaussian excitation. *Proceedings of First Pan-American Congress of Applied Mechanics, Rio de Janeiro, Brazil*, 1989.
- [10] **H.G. Davies and Q. Liu** The response probability density function of a Duffing oscillator with random narrow band excitation. *J. Sound and Vibration*, 139:1-8, 1990.
- [11] **H.G. Davies and D. Nandall** Phase plane for narrow band random excitation of a Duffing oscillator. *J. Sound and Vibration*, 104:277-283, 1986.
- [12] **M.F. Dimentberg** Oscillations of a system with a nonlinear cubic characteristic under narrowband excitation. *Mekh. Tverdogo*, 6:1404-1411, 1970.
- [13] **T. Fang and E.H. Dowell** Numerical simulations of jump phenomena in stable Duffing systems. *Int. J. of Nonlinear Mechanics*, 22:267- 274, 1987.
- [14] **R. Seydel** *From Equilibrium to chaos - Practical bifurcation and stability analysis*. Elsevier Science Publishing Co., Inc., 1988.
- [15] **W.V. Wedig** Invariant measures and Lyapunov exponents for generalized parameter fluctuations. *Struct. Safety*, 8:13-25, 1990.
- [16] **Carl de Boor** *A Practical Guide to Splines*, volume 27. Springer-Verlag New York INC., 1978.